MECHANICAL AND PERFORMANCE TESTING METHOD OF AN INTEGRATED HIGH-SPEED MOTOR COMPRESSOR

by

Thomas Alban
Research & Development Mechanical Engineer

Olivier Pellerin
Product Manager

Pierre Laboube
Research & Development Manager
GE Oil&Gas
Le Creusot, France

Bernard Quoix
Head of Rotating Machinery Department

Alain Gelin
Senior Rotating Machinery Engineer
TOTAL EP
Pau, France
and
Matthieu Oliva
Calculation Department Engineer
S2M
St Marcel, France

Thomas Alban has been Research & Development Mechanical Engineer, for GE Oil&Gas in Le Creusot, France, since 2008. He leads conceptual and mechanical design activities for part centrifugal compressors and steam turbines New Product Introduction programs. He originally joined then GE Oil&Gas Thermodyn, as Research & Development Engineer, and deeply contributed to the technical development and market introduction of the integrated compressor line product.

Mr. Alban received his Master's degree (Mechanical Engineering with specialization in turbomachinery, 2004) from Ecole Centrale de Lyon.

Olivier Pellerin has been Product Leader for GE Oil&Gas, in Le Creusot, France, for two years, leveraging 10 years of experience to develop an integrated compressor line. He started his career spending three years in the Thermodyn centrifugal compressor design department, then he joined Sundyne Corporation as a Thermodynamics and Application Engineer for six years.

Mr. Pellerin graduated (Aerodynamics Engineering, 1997) from École Nationale Supérieure de Mécanique et d'Aérotechniques.

Pierre Laboube is the Research & Development Manager of GE Oil & Gas, Thermodyn, in Le Creusot, France. Before joining Thermodyn , he was lecturer at Bath University. His career in Thermodyn began in 1974. He had several roles in the company as Application Engineer, Projects Manager, Scheduling Manager, and Applications Engineering Manager. Then, he moved from Products Leadership and Marketing to Engineering and his present position.

Mr. Laboube is an engineer graduated from Ecole Nationale des Arts et Métiers.

Alain Gelin is a Senior Rotating Equipment Engineer for Total E&P, in Pau, France. He joined Total in 2005, and he is involved in projects requiring turbomachines such as compressors, gas turbines, and pumps, and he also supports site activities. Dr. Gelin began his career in General Electric Oil&Gas (Thermodyn), Le Creusot, France, where he was the mechanical leader of the Research & Development Department from 1990 to 2002 before joining the Testing Department. He was responsible for the mechanical design of centrifugal compressors and steam turbines. During those 15 years, he was also in charge of the noise and vibration performances for all steam turbines supplied by Thermodyn for French Navy submarines.

Dr. Gelin received his B.S. degree (Mechanical Engineering, 1986) and his Ph.D. degree (Mechanical Engineering, 1990) from Institut National des Sciences Appliquées, in Lyon, France, where his research focused on rotordynamics and magnetic bearings for centrifugal compressors. He has authored or coauthored five technical papers.

Bernard Quoix is the Head of Total E&P Rotating Machinery Department, in Pau, France, and has held this position since November 2003. He began his career in 1979 within Total Operations in the North Sea, then from 1986 to 1989 became Head of Engineering of Turbomeca Industrial Division, a small and medium size gas turbine manufacturer. Mr. Quoix then went to Renault as Assistant Manager of the testing facilities for prototype and

production engines before joining Elf Aquitaine and, eventually, Total, where he was mainly involved in all aspects of turbomachines, including conceptual studies and projects for new oil and gas field development, bringing his expertise to all Total Affiliates Operations.

Mr. Quoix graduated from Ecole Nationale Supérieure d'Electricité et de Mécanique (1978), in Nancy, and then completed his engineering education with one additional year at Ecole Nationale du Pétrole et des Moteurs, in Paris, specializing in internal combustion engines.

ABSTRACT

The integrated electrical motocompressor is a recently available technology that has the advantage of drastically simplifying the machine configuration. The use of a high speed electrical motor in the process gas combined with active magnetic bearings eliminates the dry gas seals and replaces the traditional oil bearings and lube oil circuit. In addition, main auxiliaries can be avoided since the motor cooling system uses the compressor process gas as the cooling medium, making the overall package very simple. As this specific arrangement of the machine cannot be tested and validated as a conventional compressor, a validation test must take care of both the compressor and the motor.

On the mechanical standpoint, the use of active magnetic bearings (AMBs) has to be considered. It is well known that AMB characteristics differ from oil bearings in terms of damping and stiffness. This paper addresses specific limitation relative to AMBs and mainly nonlinear phenomena like magnetic material or power electronics saturation. The paper also proposes factory acceptance criteria related to this technology.

On the performance standpoint, there are no existing guidelines or standards for determining the thermodynamics performance of such systems. This paper describes the testing methodology of an integrated motor compressor to meet the ASME PTC-10 (1997) requirements.

Finally the paper will provide guidelines for comparing the overall performances of the integrated solution compared to a conventional compressor train.

INTRODUCTION

An integrated compressor is a recent known technology that becomes more and more popular as it increases the safety of the plant while decreasing gas emissions. This has been achieved by combining two main technologies: high-speed electrical motors and magnetic bearings. The use of high-speed electrical motors eliminates the requirement for gears to drive the centrifugal compressors at the optimum speed, while having the complete shaft line levitated by magnetic bearings removes the requirement of a lube oil system. These technologies have been available for more than 20 years, but the cost of dry gas seals and magnetic bearings minimized the associated expected benefits. By including the electrical motor inside the compressor casing and using the process gas as cooling medium, the dry gas seal system is no longer required.

This leads to a new generation of centrifugal compressors, being almost auxiliary free, producing zero leakage, and significantly increasing the safety. ASME PTC-10 code (1997) is widely used to measure the centrifugal compressor's performance, while API 617 (2002) governs the mechanical behavior. However, API 617 does not cover centrifugal compressors levitated by magnetic bearings while ASME PTC-10 does not consider the specific thermodynamic behavior of integrated compressors.

Following the development of a full-scale prototype, this paper proposes a methodology for mechanical and performance testing in order to validate the behavior of such compressor configuration.

BEARING TECHNOLOGIES COMPARISON

Integrated high speed motocompressors take advantage of the latest active magnetic bearings technology for shaft axial and radial displacement control. Conventional lubricated bearing performances differ from magnetic bearings, which are limited by the control loop components nonlinearities (electromagnetic actuator and power electronics). In terms of performance comparison, both static and dynamic capabilities must be investigated.

For magnetic bearings, the specific carrying static force is limited by saturation flux density B_{sat} of the magnetic laminations. The bearing load capacity per axis F_{max} can be determined as follows:

$$F_{max} = \frac{B_{sat}{}^2 A_g}{2 \mu_0} \qquad (1)$$

The two action axes of each radial bearing are oriented respectively at $-45°$ and $+45°$ versus the vertical direction to overcome the suspended weight $W/\sqrt{2}$. Each action axis should consequently generate a force parallel to the action line, directed from bottom to top, with amplitude equal to. However these values are given assuming that the maximum current I_{max} is used to carry constant loads only, with no capability to generate dynamic forces. As a design rule, up to half of this maximum current is used to withstand the static load while the remaining part is used to control the dynamic loads. Consequently, maximum bearing specific pressure P_{max} is as follows:

$$P_{max} = \frac{W_{max}}{L\,D} = \frac{B_{sat}{}^2 A_g}{\sqrt{2}\,L\,D\,\mu_0} \qquad (2)$$

For iron-silicon (Fe-3%Si) materials, the saturation is reached with a flux density of about 1.5 Tesla, giving a maximum specific pressure of 0.5 MPa according to Equation (2). Replacing these materials by cobalt-alloys increases the saturation magnetic flux density to 1.9 Tesla, leading to a maximum specific pressure of 0.8 MPa. As a matter of fact, oil lubricated bearings exhibit a maximum allowable design specific pressure in the range of 1.4 MPa (load-on-pad) to 2.2 MPa (load-between-pads), roughly 3 to 5 times higher than the magnetic bearings capability.

Like other kinds of bearings, the magnetic bearing provides stiffness and damping properties. However, unlike other bearings, the stiffness and damping vary as a function of disturbance frequency. These dynamic characteristics are adapted by the controller transfer function. This transfer function should be optimized to meet the system dynamics requirement and must be taken into account in the overall machine design. However, the controller design range is drastically limited by the capabilities of the control loop components (actuator core saturation, amplifier saturation voltage, and peak current).

For a 370 kg supercritical compressor rotor supported by two AMBs (D=120 mm, L=90 mm) and operating at 11,400 rpm, the mechanical stiffness provided by the optimized controller is compared to the vertical and horizontal stiffnesses of an equivalent oil bearing (D=120 mm, L=48 mm) (Figure 1).
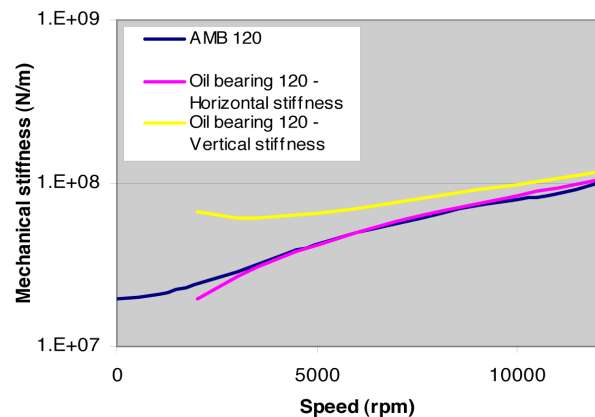

Figure 1. Dynamic Stiffness AMB/Oil Bearing.

Even if AMBs provide similar stiffnesses to conventional bearings at synchronous frequency, AMBs appear to be significantly softer at lower frequencies. Consequently, AMB's dynamic characteristics have to be tuned and optimized during the design phase by the controller within acceptable limits. Moreover, a single mechanical approach of the system is no more sufficient, and a complete mechatronic approach must be considered. It comes that any acceptance criteria referenced in common norms (API) and implicitly related to machines using lubricated bearings cannot be totally translated to machines levitated by AMBs. New criteria must be proposed and eventually agreed by all parties, mainly manufacturers and customers.

ACTIVE MAGNETIC BEARINGS OPERATION

To illustrate the behavior of a closed loop AMB/rotor system (Figure 2), and to understand the operating limits, a study case is presented. The rotor considered is the one of a full-scale prototype. This machine includes two sections of three stages each in a back to back configuration for a high pressure natural gas storage application (up to 220 bar/3190 psi). The rotor weight is 370 kg (816 lb), equally distributed between the two bearings. This rotor is supercritical since its free-free first bending mode appears at 140 Hz while the machine operates at 190 Hz.
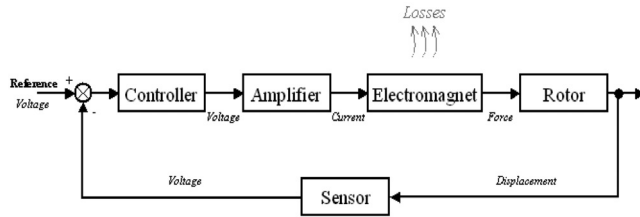

Figure 2. AMB/Rotor Closed Loop.

Figure 3. Full Scale Prototype Rotor Modeling.

The selected magnetic bearings have the following characteristics:

- Nominal diameter: 120 mm (4.72 in)

- Active laminations length: 90 mm (3.54 in)

- Nominal air gap (radial): 0.5 mm (0.02 in)

- Laminations material: Fe-3%Si

- Resulting load capacity per axis: 4 kN (900 lbf)

The power electronics characteristics are:

- Maximum delivered current: 30 A

- Amplifiers saturation voltage: 300 V

The controller transfer function of each bearing has been designed in order to have a safe closed system dynamics. Transfer functions modulus and phase variation versus disturbance frequencies are presented in Figure 4. The transfer function is based on a proportional/integral/derivative (PID) controller, the integral part minimizing the steady-state error (that is to say the gap between the position order and the resulting position) and the derivative part providing damping on the first mode. Requirements dictated by API 617 (2002) in terms of unbalance responses and shaft stability have been met.
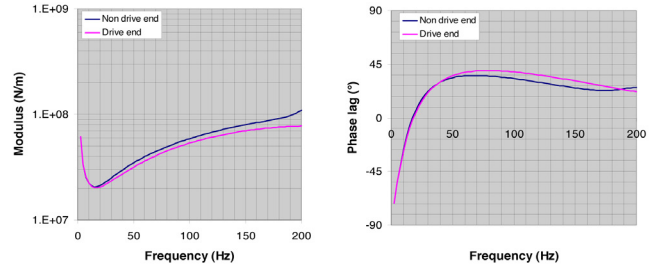

Figure 4. Bode Plots of AMB Transfer Functions.

Considering no static or dynamic loads, coils of the magnetic bearings are fed by a direct current (DC), called bias current, ensuring premagnetization of the actuators. Bias current may be continuously adapted to optimize the power consumption. For the study case a permanent bias current I_{Bias} of 10 A has been assumed.

Another DC current I_c is added to the bias current to feed the upper coils and the same value is subtracted from the bias current to feed the lower coils, generating a resulting force compensating the weight of the rotor (Figure 5). The I_c current verifies the following equation:

$$F(I_{Bias} + I_C) - F(I_{Bias} - I_C) = \frac{370 \times 9.81}{2\sqrt{2}} = 1284N\,(288\,lbf) \quad (3)$$

Using electromagnet force versus current curve, I_c is found equal to 4.85 A.
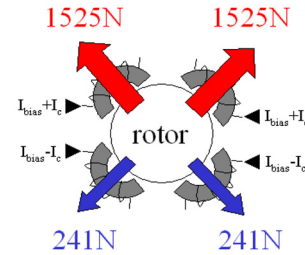

Figure 5. Static Equilibrium of Rotor in AMBs.

In addition to this static analysis, magnetic bearings have to overcome dynamic loads like:

- Unbalance forces.

- Possible aerodynamic instabilities for far off design operating conditions (impeller rotating stall, smooth diffuser stall).

- Surge.

- Large frequency band aerodynamic noise.

- Misalignment reactions.

- Etc.

As an academic example, the subject rotor running at full speed is simultaneously excited by:

- A 500 N (112.4 lbf) subsynchronous rotating force at 23.75 Hz (0.125×) corresponding to a potential aerodynamic instability.

- A 500 N (112.4 lbf) unbalance force at 190 Hz (1×) corresponding to roughly two times the API unbalance.

- A 500 N (112.4 lbf) supersynchronous rotating force at 380 Hz (2×), which could be associated to some kind of misalignment.

All the forces are applied at the center of the rotor. The resulting bearings reaction components are summarized in Table 1 (AMB1 = Non drive end bearing, AMB2 = Drive end bearing). The resulting rotor vibrations resulting from the different loads are summarized in Table 2, underlining that the orbits in the AMBs are circular when operating away from any actuator nonlinearities.

Table 1. Bearing Reactions.

	AMB 1	AMB 2
Subsynchronous force compensation (@ 0.125X)	295 N (66.3 lbf)	371 N (83.4 lbf)
Unbalance force compensation (@ 1X)	341 N (76.7 lbf)	78.7 N (17.7 lbf)
Supersynchronous force compensation (@ 2X)	152 N (34.2 lbf)	31 N (7 lbf)

Table 2. Rotor Vibrations.

	AMB 1	AMB 2
Rotor vibrations @ 0.125X	14.0 μm (0.55 mill)	17.9 μm (0.70 mill)
Rotor vibrations @ 1X	3.3 μm (0.13 mill)	0.78 μm (0.03 mill)
Rotor vibrations @ 2X	0.35 μm (0.015 mill)	0.40 μm (0.016 mill)

From these data, all the real time operating parameters of the bearings can be computed as follows:

- Actuator air gap $X(t)=X_0+x(t)$
- Coil currents $I(t)=I_0+i(t)$
- Amplifier voltages $U(t)$

This last parameter can be deduced from air gap and current parameters using the exact Equations (4) and (5):

$$U(t) = RI(t) + N\frac{d\phi(t)}{dt} \qquad (4)$$

with:

$$\phi(t) = \frac{N[I_0 + I(t)]\mu_0 A_g}{2[X_0 - x(t)]} \qquad (5)$$

The coil resistance is generally negligible (between 0.1 and 0.35 Ω) and amplifier voltage can be calculated using Equation (6):

$$U(t) \approx \frac{N\mu_0 A_g}{2}\frac{(X_0 - x(t))\frac{\partial I(t)}{\partial t} + (I_0 + I(t))\frac{\partial x(t)}{\partial t}}{(X_0 - x(t))^2} \qquad (6)$$

For one action axis of the AMB1, the operating parameters x(t), I(t), and U(t) are plotted in Figure 6 together with the associated spectra (no constant term).
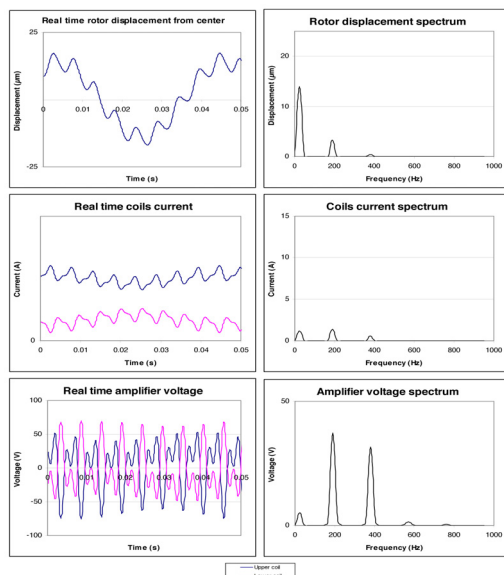

Figure 6. AMB1 Operating Parameters for One Axis.

From the plots, the following general rules can be deducted:

- The low frequency disturbance requires low feeding current (1.2 A), almost no voltage consumption (<5V) but large rotor displacements (14 μm zero-to-peak/0.55 mils zero-to-peak). In this case, the rotor/bearings system is protected by the vibration monitoring system.

- The unbalance force generates very small rotor vibrations (<4 μm zero-to-peak/<0.16 mils zero-to-peak) but leads to some voltage consumption (37 V).

- The supersynchronous disturbance leads to negligible rotor vibrations but the voltage consumption is very large with respect to the bearing control force. Indeed for an unbalance disturbance, a 341 N (76.7 lbf) bearing force leads to a voltage consumption of 37 V, while for supersynchronous disturbance, a 152 N (34.2 lbf) bearing force leads to a voltage consumption of 32 V. Generally speaking, limits for high frequency disturbances control arise from amplifier requested output voltage. Consequently, amplifier voltages also need to be monitored.

It emphasizes the fact that, depending of the disturbances nature, rotor and bearing performance limits may come from any of the operating parameters: displacement, current, voltage.
    In addition to that, the magnetic bearings generate losses, which take three forms: magnetic hysteresis, Joule, and windage effect from gas film shearing in the gap. The resulting heat must be evacuated by flushing the gap with a cooling gas, otherwise the AMBs' core may heat up and lamination performances may drop drastically. Consequently, the core temperature must be monitored as well. As a result, the rotor and bearing system is fully monitored and protected as shown in the schematic presented in Figure 7.
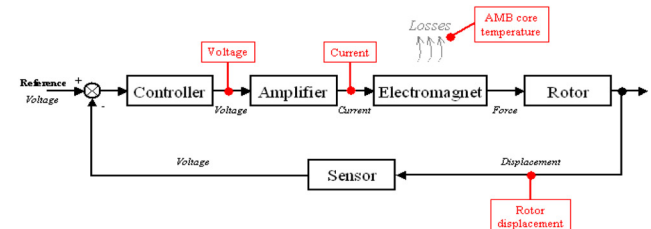

Figure 7. Rotor/AMB Full Protection Scheme.

FACTORY ACCEPTANCE CRITERIA

Each of the required parameters (voltage, current, vibrations, and temperatures) must be available during machine operation and associated factory acceptance criteria be defined.

Rotor Vibrations Limit

The vibrations limit must prevent any rotor-stator contact during operation. Consequently, the vibrations must be based on the minimum distance between rotating and stationary parts along the rotor. Basically, both axial and radial minimum clearances are set by the backup bearings. This approach is consistent with the few existing standards dealing with the AMB levitated turbomachinery.
    Indeed, general ISO 14839-2 (2004) standard proposes a criterion of $0.3C_{min}$, C_{min} being the minimum clearance between the rotor and the stator. ISO 14839-2 applies this limit to the journal bearing displacement, e.g., rotor displacement from center of the electromagnet. ISO standard proposes to use this criterion for newly commissioned machines, and referring implicitly to final field conditions. API 617, Seventh Edition (2002), annex 4F dealing with turbo expanders, provides the same rule but applies it to the rotor movement in the backup bearings. In addition, API 617 deviates from ISO 14839-2 since the limit is applied during the mechanical running test (MRT) only.

In any case, the rotor displacements in both electromagnet plane and backup bearings plane are not directly accessible since sensors ring is not collocated with any of the previous positions. Depending on the rotor deflection shape, the differences may be large. Consequently, the criterion must refer to the measurements in the sensor ring plane only.

In addition to that, the experience has shown that measured vibrations during a full load shop acceptance test are usually slightly smaller than those observed on sites, mainly because upstream and downstream equipment generate additional disturbances. The discrepancy is increased while comparing MRT and field behavior.

As a result, the 30 percent of the auxiliary bearings clearance vibration limit, measured at the sensors locations, should be applied to site conditions, while two additional levels should be considered: one for the full load shop tests, and the other for the MRT/no load shop tests. The recommended acceptance criteria are summarized in Table 3. These limits can be applied to any magnetic axis (axial and radial) of the compressor and the electrical motor.

Note: The proposed criterion considers only the rotor vibration, which is the dynamic part of the shaft movement, because position is adjusted during commissioning to have the rotor perfectly centered in the backup bearings.

Table 3. Recommended Vibration Limits.

Operating conditions	Acceptance criteria
At site	$0.3\ C_{min}$
Shop full load test	$\dfrac{0.3\,C_{min}}{1.5}$
Shop no load MRT	$\dfrac{0.3\,C_{min}}{2.0}$

The above-mentioned criterion considers the overall vibrations, which includes nonsynchronous vibrations. Due to the PID controller and the resulting electrical stiffness low modulus at low frequency, it is expected to see some wideband subsynchronous activity on this type of machine without any particular observed vibration peak. It would not appropriate to try cancelling these vibrations because it would lead to stiffen the bearings at low frequency while deteriorating other high frequency characteristics. However, these low frequency vibrations must not prevent detection of potential mechanical or aerodynamic instabilities typically resulting in a vibration peak in this frequency range. As a consequence, the spectra used for online analysis should have enough resolution (usually 1 or 2 Hz) to spread this subsynchronous activity on as many harmonics as possible to be able to observe any peak at a given frequency.

Peak Force Limit

Any magnetic material used for rotor and stator laminations has a given saturation flux density, providing a limited carrying force capability. Any overload beyond that limitation will cause large rotor displacements from its center position and may eventually lead to a hard touchdown of the rotor on its backup bearings. This must be prevented as much as possible.

Usually, AMB systems are designed so that the selected amplifiers maximum deliverable current i_{max} corresponds to the saturation flux density. It means that the ratio of real time current to i_{max} is a picture of the operating margin to saturation. Consequently, the force (or flux density) criterion should be translated in a current criterion. The recommended factory acceptance criterion is as follows:

● For all the normal operating points, the real time current in any coil of the magnetic bearings system should not exceed 80 percent of the maximum available current i_{max}.

The 20 percent remaining margin to bearing saturation can account for any evolution of the dynamic disturbances related to far off-design operating conditions or during the life of the machine.

Voltage Limit

This limitation arises from the fact that the magnet coils consume voltage by induction and that the power amplifier has a limited driving voltage level U_{max}. Regarding Equation (6), the driving voltage limitation is translated in a limited possible rate of change of the current (Figure 8). On this example, the requested current is fully achievable with a 300 V power amplifier but not with a 200 V power amplifier, and distortions occur. The distorted current signal obtained with the 200 V power amplifier contains harmonics of the fundamental frequency that could excite the rotor. This generally results in a loss of damping, which, in some cases, may destabilize the rotor. It means that in normal operation, the amplifiers should work sufficiently far away from saturation in order to have the possibility to account for potential disturbances evolution. The recommended factory acceptance criterion is as follows:

● For all the normal operating points, the real time voltage of any amplifier should not exceed 80 percent of its maximum available voltage.
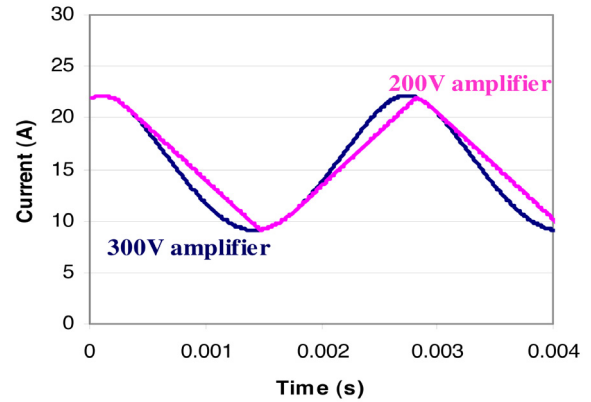

Figure 8. Effect of Amplifier Saturation.

The direct access to the real time amplifier voltage is challenging. A direct measurement is feasible with linear amplifiers but this type of component is not a standard one due to its limited current capacity. Generally AMB manufacturers integrate switched mode power amplifiers with pulse width modulation (PWM) control (Figure 9).
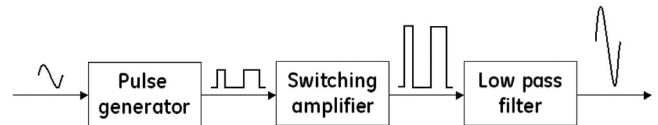

Figure 9. PWM Amplifier Block Diagram.

Usually control cabinets are not equipped with accurate voltage sensors at the outlet of the amplifiers and the implementation of such devices would require extensive modifications. Most reasonably, the voltage should be obtained from other available operating parameters using equation (6). Generally speaking, the feeding currents can be easily measured using induction sensors located on the wires between the control cabinet and the motor compressor. However, the electromagnet air gap $X_0 - x(t)$ is not accurately measured since magnetic bearings sensor rings are not collocated with the bearing centerline. Assuming that the deviation x from nominal gap distance remains small and that the coil resistance is negligible, the equation can be simplified as follows:

$$U(t) \approx \frac{N^2 \mu_0 A_g}{2\ X_0} \frac{dI(t)}{dt} = L_0 \frac{dI(t)}{dt} \tag{7}$$

with L_0 being the bearing nominal inductance or small displacement inductance.

Taking an example combining synchronous and nonsynchronous disturbances, resulting in a peak-to-peak vibration of say 60 μm in the center of the bearing, the discrepancy between the real amplifier voltage and the voltage obtained from Equation (7) is 13 V only (Figure 10). Compared to the amplifier maximum available voltage of 300 V, it represents 4.3 percent, which is fully acceptable.
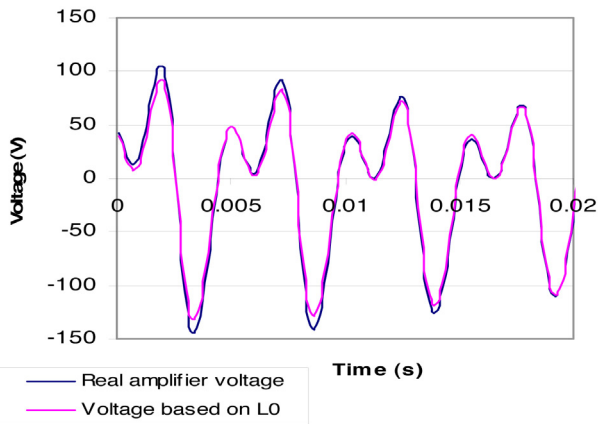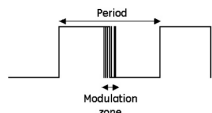

Figure 10. Comparison Between Real Voltage and Voltage Estimated with Equation (7).

Some bearing manufacturers have access to a picture of the pulsed signal in between the pulse generator and the switching amplifier. A modulation rate MR can be defined as shown in Figure 11.

$$MR = \frac{Modulation\ zone}{Period}$$

Figure 11. Modulation Rate MR.

A 100 percent modulation rate means the amplifier does not switch to its low level during at least one period and consequently the maximum output voltage is temporarily reached. With this method, the voltage acceptance criterion can be expressed in the following way:

• For all the normal operating points, the modulation rate of any amplifier should not exceed 80 percent.

Actuator Core Temperature Limit

The bearing cooling flow is adapted to the bearing design temperature class. Generally, insulation class of AMBs for motocompressors is F or H, according to NEMA standards (Table 4). Bearings cooling flow is negligible compared to the main gas flow. The cooling flow can be increased with a limited impact on the overall machine performance and the following acceptance criteria can be verified:

• For all the normal operating points, bearings core continuous temperature should not exceed the maximum average temperature of the subject insulation class minus 40°C (104°F).

Table 4. NEMA Insulation Classes F & H.

	Class F	Class H
Maximum average temperature	145°C (293°F)	165°C (329°F)
Maximum hot spot temperature	155°C (311°F)	180°C (356°F)

PROTOTYPE FULL LOAD TESTING

A full-scale prototype has been extensively tested to validate the product concept under full load conditions (full speed, full power, full pressure) using natural gas. Mechanical behavior of the machine has been checked. The acceptance criteria proposed in this paper were applied to check the operation at the design point (Figure 12).

Figure 12. Recorded Vibrations on Compressor (Suction Pressure 50 Bar, N=12,000 RPM).

Mechanical Performance

The compressor vibrations analysis shows a very stable behavior of the machine with a peak-to-peak vibration remaining below 30 μm (1.2 mils) (Figure 13), while the above-mentioned criterion gives a 60 μm (2.4 mils) peak-to-peak as an acceptable overall vibration. As expected, some low frequency vibration activity appears, with a very limited amplitude level.
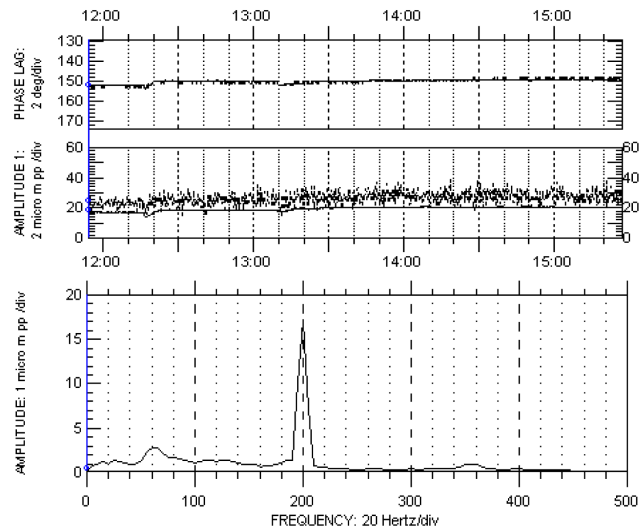

Figure 13. Compressor Bearings' Temperatures.

Real time currents and voltages were not recorded during the test campaign. However, performed tests showed the need to have such criteria on currents and voltages in order to understand the available margins.

Two temperature probes were installed on each AMB. The AMB insulation class is H and the measured temperatures should not exceed 125°C (257°F), according to the proposed criterion. Figure 14 shows the temperature parameter variations from standstill to full speed, and then from stonewall limit to surge limit. At any time, the temperature remained well below 90°C (194°F), including during transient operating conditions.
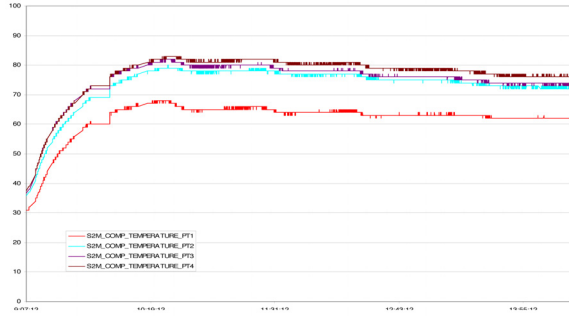
Figure 14. *Control Volume of Complete Integrated Electrical Motor Compressor.*

THERMODYNAMIC BEHAVIOR OF AN INTEGRATED MOTOR COMPRESSOR IN BACK-TO-BACK CONFIGURATION

Compared to conventional compressors, the integrated machines require additional flow gas paths to cool down the electrical motor and the active magnetic bearings. The heat dissipation by natural convection and radiation can be neglected (in the range of ~15 kW/20 hp compared to 4000 to 15,000 kW/5300 to 20,000 hp), and as a consequence, the system could be considered as adiabatic and the process gas evacuates all the losses from the magnetic bearings, the motor, and the compressor.

Considering the complete machine volume control (Figure 15— Purple: Compressor main flow gas path; Blue: Electrical cooling recirculation flow path; Red: Balance drum recirculation), the only input and output between the control volume of the integrated motor compressor are the customer main connections. Compared to a conventional compressor, the flange-to-flange efficiency of the integrated motor compressor includes all the losses.

- Compressor stages efficiency
- Internal leakages (internal labyrinths and balance drum)
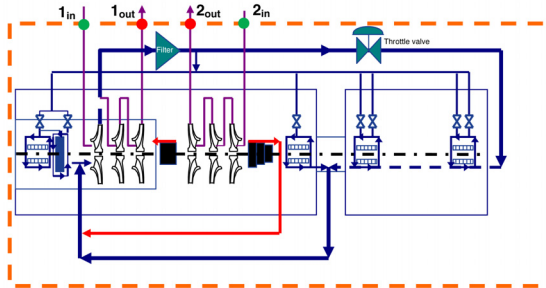- Motor losses
- Active magnetic bearing losses

Figure 15. *Cooling Flow Schematic.*

The compressor stage losses come from the centrifugal compression technology; the internal leakages are mainly related to the recirculation through the balance drum. They are similar to the ones of a conventional centrifugal compressor.

What is new in an integrated motor compressor is the use of the process gas for cooling purposes. The process gas is used to cool down all electrical parts, meaning that the motor efficiency and the power dissipated in the magnetic bearings affect directly the compressor flange-to-flange performances.

Impact of Cooling System on Compressor Performances

As shown in Figure 16, a part of the main flow is extracted at the exit of the first impeller and is used to feed and cool both the motor and the AMBs. All the cooling flows are brought back to the inlet of the compressor:

- The electrical motor cooling flow and the cooling flows of the centrifugal compressor drive end (CC DE), electrical motor drive end (EM DE), and nondrive end (EM NDE) bearings through the balance line,

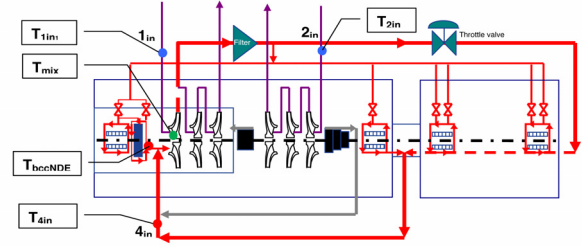- The cooling flow of the centrifugal compressor nondrive end (CC NDE) bearing.

Figure 16. *Control Volume of Complete Integrated Motor Compressor with External Cooling.*

As a matter of fact, the cooling flow requirement is mostly driven by the electrical motor and is one order of magnitude greater than the one requested by all the magnetic bearings. To optimize the overall efficiency of the system on the complete compressor field with a simple cooling system, one control valve is installed on the electrical motor cooling line that controls its own cooling flow while all magnetic bearing cooling flows are determined by means of calibrated orifices. This extracted flow, once used to cool down the electrical parts, comes back to the first impeller inlet and is mixed with the main inlet gas flow from compressor inlet main connection.

At the first impeller inlet, the flow includes the following:

- Specified process mass flow
- Electrical cooling mass flow (from the electrical motor and AMBs)
- Balance drum mass flow (recirculation)

The resulting internal inlet temperature is calculated using the following equation:

$$(H_{T_{mix}} - H_{T_{1in}}) \times \dot{m}_{cust} + (H_{Tmix} - H_{T_{4in}}) \times (\dot{m}_{EM} + \dot{m}_{bem} + \dot{m}_{bccDE}) + (H_{T_{mix}} - H_{TbccNDE}) \times \dot{m}_{bccNDE} + (H_{Tmix} - H_{T_{2in}}) \times \dot{m}_{lf} = 0 \tag{8}$$

In this equation, the inlet temperature of the main flow at flange location, and the gas temperature from the balance line can be measured during the test, while the CC-NDE bearing return temperature has to be calculated using bearing losses prediction. This has a minor impact on the mixing temperature, as the NDE cooling flow is low compared to the other ones. The assumption is made that the final balance drum leakage is isenthalpic, so the massic enthalpy coming from the balance line is equal to the one coming from the second stage main inlet.

This arrangement has a main impact in the design of the compressor: the first impeller has to be over-designed in order to handle this recirculation flow. Depending on the customer flow, temperature and pressure, the cooling flow could typically reach 5 to 15 percent of the design flow leading to an oversizing of the first impeller accordingly.

The increase of the first impeller inlet temperature, due to all electrical losses, directly impacts the measured efficiency of the first section of the compressor and explains the degradation of the flange-to-flange efficiency compared to an equivalent conventional centrifugal compressor section.

To summarize, the first stage efficiency is decreased by the flow recirculation around the first impeller and the heat generated by the electrical losses. The total power of the integrated compressor, including electrical losses, is thus defined by:

$$P = H_{1out} \times \dot{m}_{1out} - H_{1in} \times \dot{m}_{1in} + H_{2out} \times \dot{m}_{2out} - H_{2in} \times \dot{m}_{2in} \tag{9}$$

This power includes all the losses coming from the magnetic bearings and the electrical motor.

Optional Cooler on the Balance Line

A cooler could be added in the system to cool down the flow of the balance line. This will drop the temperature down at the first impeller inlet accordingly and will reduce the required head to be developed by the first section of the compressor for a given pressure ratio. Figure 17 illustrates its installation within the overall system.
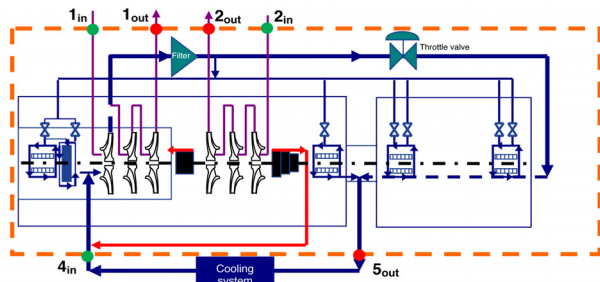

Figure 17. Comparison of Gas Power and Electrical Power During Full Load Test.

Keeping the control volume method, the power computation has to be modified adding one extra input and one extra output for the heat removal of the balance line. The total power of the integrated compressor, including electrical losses, need to take care of the cooling system. The power balance equation becomes:

$$P = H_{1out} \times \dot{m}_{1out} - H_{1in} \times \dot{m}_{1in} + H_{2out} \times \dot{m}_{2out} - H_{2in} \times \dot{m}_{2in} +$$
$$(H_{5out} - H_{4in}) \times (\dot{m}_{bemNDE} + \dot{m}_{bemDE} + \dot{m}_{bccDE} + \dot{m}_{EM}) \quad (10)$$

Using the following equations:

$$P_1 = (H_{1out} - H_{1in}) \times \dot{m}_{cust} \quad (11)$$

$$P_2 = (H_{2out} - H_{2in}) \times \dot{m}_{cust} \quad (12)$$

$$P_{leakage} = (H_{1out} - H_{2in}) \times (\dot{m}_{li} + \dot{m}_{lf}) \quad (13)$$

$$P_{cooler} = (H_{5out} - H_{4in}) \times (\dot{m}_{bemNDE} + \dot{m}_{bemDE} + \dot{m}_{bccDE} + \dot{m}_{EM}) \quad (14)$$

Equation (10) becomes:

$$P = P_1 + P_2 + P_{cooler} + P_{leakage} \quad (15)$$

Equation (15) remains valid, even when there is no cooling system.

FULL LOAD TEST FOR
PERFORMANCE VALIDATION
ACCORDING TO ASME PTC-10 TYPE 1

The purpose of this test is to demonstrate the satisfactory operation of a full-scale integrated motor compressor and its auxiliary systems when operating at full speed, full load, and full pressure conditions. The sequences include thermodynamic performance tests while the motor is running at full power.

The scope of the tested equipment should be clearly defined. Here this scope will be limited to the compressor package only, that means for the integrated motor compressor:

• Compressor, motor, and coupling

• Train and auxiliary equipment instrumentation of the compressor and the motor package such as temperature, flow, and pressure transmitters

• Balance line cooler when applicable.

Like any other compressor, the full load test will take care of the flange-to-flange performance of the integrated compressor, using the same method. In this particular case, the heat balance method (ASME PTC-10 Section 4.15, 1997) is used to check the integrated compressor behavior. The customer conditions are used for such a test, and no specific caution is to be considered with regard to the integrated machine. The motor and the compressor are tested together in real conditions.

Depending on the accuracy of the power measurement on the variable frequency drive, the electrical power can confirm the measured gas power. During the full load test campaign of the pilot unit, the comparison has been performed, as shown in Figure 18.
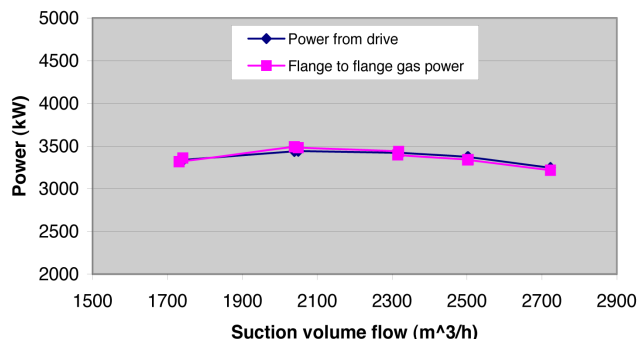

Figure 18. Allowable Machine Mach Number Departures.

LOW SPEED LOW-PRESSURE PERFORMANCE
TEST ACCORDING TO ASME PTC-10 TYPE 2

The purpose of the ASME PTC-10 (1997) type 2 tests is to validate the compressor performance using gas in similitude conditions. Typically this test is done using an inert gas at reduced speed and pressure. The application of the proper similitude conditions allows getting an accurate measurement of thermodynamic performances. The paper will present how the ASME PTC-10 type 2 test could be performed to measure the thermodynamic performances of an integrated motor compressor.

The purpose of the type 2 test is to provide the compressor dimensionless curves and parameters:

• Pressure coefficient versus flow coefficient

• Polytropic efficiency versus flow coefficient

Flow and pressure coefficients are defined by the following formula:

Flow coefficient:

$$\phi = \frac{240.Q_s}{\Pi^2 . D_s^{\ 3} . N} \quad (16)$$

Pressure coefficient:

$$\psi = \frac{\dfrac{H_p}{n}}{\left(\dfrac{D_a.N}{60}\right)^2} \quad (17)$$

with:
Qs   = Suction volume flow (m^3/s)
Ds   = Standard impeller diameter (m)
N   = Rotating speed (rpm)
Hp   = Section polytropic head (J/kg)
n   = Number of impellers per section
Da   = Average actual impeller diameter (m)

At the guaranteed points, the dimensionless parameters must match the customer conditions with accuracy (per ASME PTC-10 type 2, 1997) as shown in Table 5 and Figures 19 and 20.

Table 5. Min and Max Code Limits.

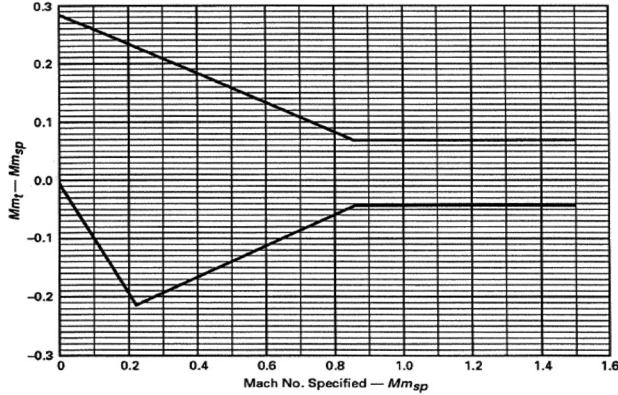|		Min and max code limits in % of the nominal point value	
- Volume flow ratio	Qs/Qd	95	105
- Flow/speed ratio	Qs/N	96	104
- Reynolds number	Rem	See Figure 19	
- Mach number	Mm	See Figure 20	

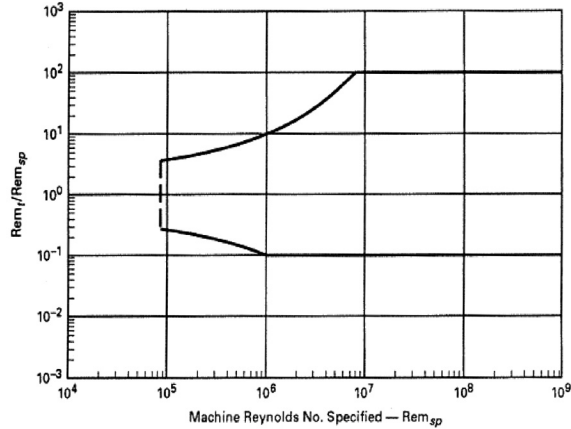Figure 19. Allowable Machine Reynolds Number Departures.

Figure 20. Compressor Only Control Volume.

The electrical motor being used for the type 2 test, the cooling flow extraction, has an impact on the first impeller design, which also impacts the performances. Therefore, it is mandatory to take care of this recirculation in case of ASME PTC-10 type 2 test.

In general, the similitude test uses inert gas or a mixture of inert gases, normally with different molecular weight, and the test is conducted at lower speed and pressure. In these conditions, the motor power and losses will be significantly different from the nominal ones and thus cannot be considered as such while performing the ASME PTC-10 type 2 test. To carry out a proper ASME PTC-10 type 2 test on an integrated motor compressor, precautions must be taken on the motor cooling loop.

The easiest way to get around this unavoidable fact is to separate the cooling flow for the electrical motor and magnetic bearings from the main compressor gas flow, while keeping extraction in similitude conditions at the exit of the first impeller of the compressor. All these steps are explained in detail below.

The first step is to isolate the motor influence and to define similitude conditions corresponding to the operating conditions. A new control volume has to be defined to remove the motor influence as shown in Figure 21.
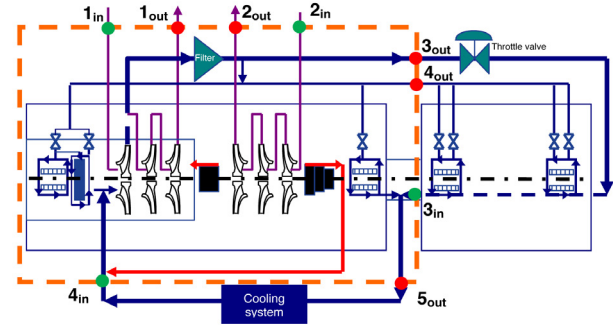

Figure 21. Test Loop Configuration.

Using the control volume of Figure 21, excluding the electrical motor, the compressor shaft power can be measured as follows:

$$P_{shaft} = H_{1out} \times \dot{m}_{1out} - H_{1in} \times \dot{m}_{1in} + H_{2out} \times \dot{m}_{2out} - H_{2in} \times \dot{m}_{2in}$$
$$+ (H_{5out} - H_{4in}) \times (\dot{m}_{bemNDE} + \dot{m}_{bemDE} + \dot{m}_{bccDE} + \dot{m}_{EM}) \qquad (18)$$
$$+ (H_{3out} - H_{3in}) \times \dot{m}_{EM} + (H_{4out} - H_{3in}) \times (\dot{m}_{bemDE} + \dot{m}_{bemNDE})$$

The motor losses include:

- The electrical losses and the windage effect from the motor.
- The electrical losses and windage effect from the motor bearings.

Thus the motor power losses are defined by:

$$P_{Motor} = -(H_{3out} - H_{3in}) \times \dot{m}_{EM} - (H_{4out} - H_{3in}) \times (\dot{m}_{bemDE} + \dot{m}_{bemNDE}) \quad (19)$$

The integrated compressor shaft power Equation (18) becomes, using Equations (11), (12), (13), (14), and (19):

$$P_{shaft} = P_1 + P_2 - P_{Motor} + P_{cooler} + P_{leakage} \qquad (20)$$

The heating power of the first stage is:

$$P_{heating} = P_{Motor} - P_{cooler} \qquad (21)$$

To perform the test, the similitude conditions should be established at:

- The customer main flange connections,
- The cooling extraction flange,
- The first impeller inlet.

Definition of Customer Conditions

At the main flange connections, the customer pressure, temperature, and flow are given by the process datasheet. But for the electrical motor cooling flow and the leakage recirculation, the parameters are dictated by the manufacturer. The impeller inlet pressure p_{mix} is defined using the momentum conservation from all entering flows, while the inlet temperature t_{mix} is defined using Equation (8). The inlet mass flow at the first impeller is then given by:

$$\dot{m}_{mix} = \dot{m}_{cust} + \dot{m}_{cust} + \dot{m}_{lf} \qquad (22)$$

The conditions coming from the customer are the following:

Stage 1 inlet pressure
$\quad p_{s1}$
Stage 1 inlet temperature
$\quad t_{s1}$
Stage 1 inlet mass flow
$\quad \dot{m}_{cust}$
Stage 1 inlet volume flow
$\quad Qs_1$

Stage 1 discharge volume flow
Qd_1
Stage 1 discharge pressure
p_{d1}
Stage 1 inlet Machine Mach number
Mm_1
Impeller 1 inlet pressure
p_{mix}
Impeller 1 inlet temperature
t_{mix}
Impeller 1 inlet mass flow
$\dot{m}_{mix}$
Impeller 1 inlet volume flow
Qs_{mix}
Impeller 1 inlet Machine Mach number
Mm_{mix}
Compressor speed
N
Stage 2 inlet pressure
p_{s1}
Stage 2 inlet temperature
t_{s1}
Stage 2 inlet mass flow
$\dot{m}_{cust}$
Stage 2 inlet volume flow
Qs_2
Stage 2 discharge volume flow
Qd_2
Stage 2 discharge pressure
p_{d2}
Stage 2 inlet Machine Mach number
Mm_2

As a conclusion of this chapter the similitude parameters remain the usual ones for the first and second stages:

Volume flow ratio at stage 1 flange
Qs_1/Qd_1
Flow/speed ratio at stage 1 flange
Qs_1/N
Reynolds number at stage 1 flange
Rem_1
Mach number stage 1 flange
Mm_1
Volume flow ratio at stage 2 flange
Qs_2/Qd_2
Flow/speed ratio at stage 2 flange
Qs_2/N
Reynolds number at stage 2 flange
Rem_2
Mach number stage 2 flange
Mm_2

But, to take into account the actual operating conditions of the first impeller, the following additional similitude parameters are proposed:

Flow/speed ratio at first stage inlet
Qs_{mix}/N
Reynolds number at first stage inlet
Rem_{mix}
Mach number at first stage inlet
Mm_{mix}

Similitude Principle for Integrated Motor Compressor in Back-to-back Arrangement

In order to control the compressor performances, the motor needs to be cooled separately and the impact has to be properly integrated in the compressor performances calculation. Figure 21 shows the two separate loops that allow the similitude test:

• The first one simulates the cooling recirculation and ensures the similitude condition at the first impeller inlet.

• The second one cools the motor during the test. This is fed by the exit of the second stage without impacting the performance measurement of the second stage. As shown in Figure 22, a third cooler is used and dedicated to cool down the extraction of stage 2 loop for the motor cooling, while cooler 2 takes care of the complete flow entering in stage 2.
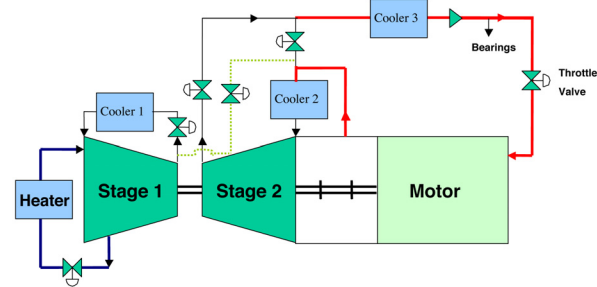

Figure 22. Test Loop Control Volume.

Stage 1 Cooling Loop Simulation

To simulate the electrical motor and AMB losses, a recirculation loop is created between stage 1 first impeller extraction and compressor main inlet. On this loop, a control valve adjusts the flow to simulate the required mass flow in order to have the first impeller seeing the extra volume flow generated by the cooling recirculation in similitude condition. A heater emulates the heating power generated by the electrical motor plus the optional cooler. The heating power ratio shall be kept constant between the gas power of section 1 at similitude conditions and the same at customer conditions. This is the last similitude parameter that must be carefully checked.

$$\frac{P_{Heater}}{P_{1\_Sim}} = \frac{P_{Heating}}{P_1} \qquad (23)$$

The electrical motor losses are function of speed, inlet pressure, and electrical power. At constant speed and inlet conditions, the cooling flow recirculation and the generated heat are just a function of the electrical power. Extracted mass flow and generated heat are controlled during all test points to remain in the similitude conditions.

Test Loop Configuration

As shown in Figure 23, the mass flow balance between stage 1 and stage 2 loops is achieved with a dedicated shop test balance line that compensates the NDE compressor bearing cooling mass flow and the balance drum leakage flow. The equalization is made by tuning the shop test balance line control valve in order to stabilize the mass flow in the system.
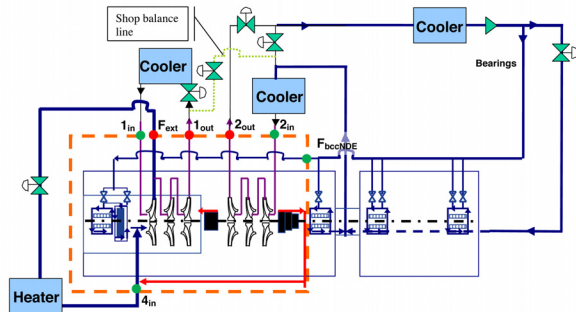

Figure 23. Similitude Parameters.

In all conditions (similitude and customer conditions), the NDE compressor bearing cooling mass flow is very small compared to

the extracted cooling mass flow; it represents less than 5 percent of the extracted flow and less than 0.5 percent of the inlet flange mass flow. Consequently, the mass flow of the NDE compressor bearing can be neglected and the cooling loop of the electrical motor is considered separately. Using Figure 23 control volume, the shaft power is defined by:

$$P_{Shaft\_sim} = H_{1out\_sim} \times \dot{m}_{1out\_sim} - H_{1in\_sim} \times \dot{m}_{1in\_sim} + H_{2out\_sim} \times \dot{m}_{2out\_sim} - H_{2in\_sim} \times \dot{m}_{2in\_sim} + H_{Fext\_sim} \times \dot{m}_{ext\_sim} - H_{4in\_sim} \times \dot{m}_{4in\_sim} - H_{FbccNDE\_sim} \times \dot{m}_{FbccNDE\_sim} \quad (24)$$

Assuming that the NDE compressor bearing losses are very small compared to the other losses, Equation (24) becomes:

$$P_{Shaft\_sim} = H_{1out\_sim} \times \dot{m}_{1out\_sim} - H_{1in\_sim} \times \dot{m}_{1in\_sim} + H_{2out\_sim} \times \dot{m}_{2out\_sim} - H_{2in\_sim} \times \dot{m}_{2in\_sim} + \left(H_{Fext\_sim} - H_{4in\_sim}\right) \times \dot{m}_{ext\_sim} \quad (25)$$

The heating power introduced in stage 1 during similitude test conditions to simulate the electrical losses can be written as follows:

$$P_{Heater} = \left(H_{Fext\_sim} - H_{4in\_sim}\right) \times \dot{m}_{ext\_sim} \quad (26)$$

Using Equations (11), (12), (13), and (26), the shaft power in similitude conditions is given by:

$$P_{Shaft\_sim} = P_{1\_sim} + P_{2\_sim} + P_{leakage\_sim} + P_{Heater} \quad (27)$$

The measurement in similitude conditions of the mass flows and the pressures and temperatures at inlet and discharge flanges allow defining the stages behavior and computing the dimensionless aerodynamics parameters and curves. Then, as for a conventional compressor, these curves are used to generate the as-built performances at customer conditions as per ASME PTC-10 code.

Proposed Similitude Parameters

Taking care of the specificity of integrated motor compressors, the following similitude parameters have to be checked during the ASME PTC-10 type 2 tests:

Volume flow ratio at stage 1 flange
Qs_1/Qd_1 ±5%
Flow/speed ratio at stage 1 flange
Qs_1/N ±4%
Reynolds number at stage 1 flange
Rem_1 see table
Mach number stage 1 flange
Mm_1 see table
Volume flow ratio at stage 2 flange
Qs_2/Qd_2 ±5%
Flow/speed ratio at stage 2 flange
Qs_2/N ±4%
Reynolds number at stage 2 flange
Rem_2 ±5%
Mach number stage 2 flange
Mm_2 ±5%
Flow/speed ratio at first stage inlet
Qs_{mix}/N ±4%
Reynolds number at first stage inlet
Rem_{mix} see table
Mach number at first stage inlet
Mm_{mix} see table
Heating power ratio

$$\frac{P_{Heating}}{P_1} \quad ±4\%$$

FULL SCALE PROTOTYPE THERMODYNAMICS PERFORMANCE RETURN OF EXPERIENCE

The above presented approach of similitude condition results from the pilot unit experimental program comparison between the full load test thermodynamics performance with natural gas and the similitude performance with CO_2 using the same testing set up (without considering the proper similitude conditions for the electrical motor).

During the test campaign, a similitude test was performed, using the standard test set up conditions of ASME PTC-10 type 2. Figure 24 shows that both sections, and almost all stages, remained within similitude conditions according to ASME PTC-10 criteria.
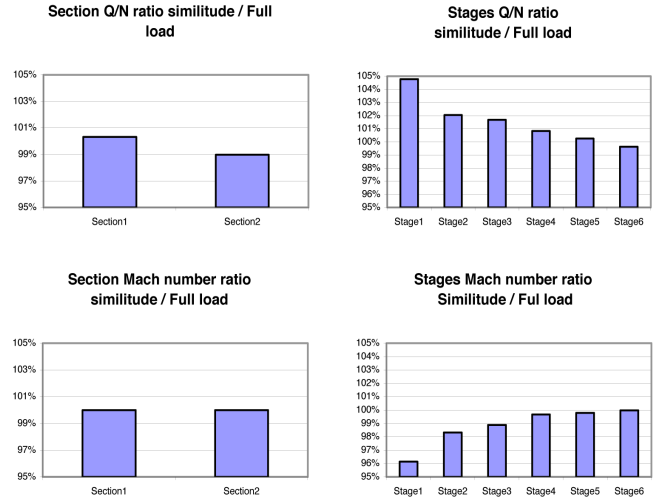

Figure 24. Dimensionless Performance Ratio.

Looking at Figure 25, it appears for the second section, both flange-to-flange measured performances and resulting individual stages calculated performances are very accurate, either at full load type 1 or in similitude type 2 conditions (<0.2 percent difference in head and efficiency). The first section shows unacceptable flange to flange results: 3.5 percent in head and 7.5 percent in efficiency, while the resulting individual stages calculated performances are more accurate in terms of efficiency (<1 percent difference in efficiency).
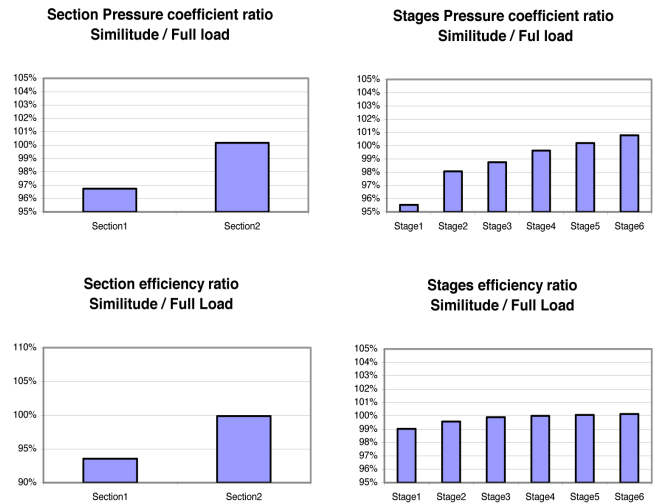

Figure 25. Heating Power Ratio.

Figure 26 shows the poor similitude conditions that create such a difference during the prototype test. This clearly demonstrates that the heat generated by the electric motor shall also be considered

in similitude conditions, as proposed by the new testing approach proposed in this paper.
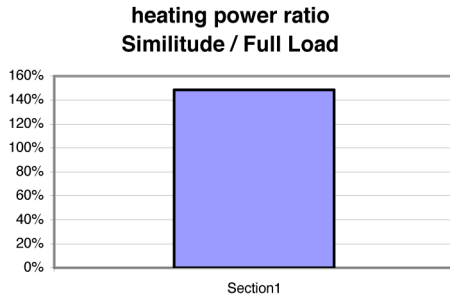

Figure 26. Mass Flow Definition.

CONCLUSION

First of all, this paper emphasizes that integrated electrical motor compressors cannot be directly compared with conventional centrifugal compressors due to their specific design. Both mechanical and thermodynamics criteria have to be reviewed.

On the mechanical standpoint, the use of active magnetic bearings instead of conventional bearings is the main design change. The existing standards do not fully cover the subject. Historically the approach is purely mechanical while the use of active magnetic bearings shall include mechanical, electromagnetism, and power electronics related aspects. This paper proposes acceptance criteria that include all these aspects.

About the performances, the main deviation compared to conventional compressors is that the measured flange-to-flange gas power includes all the losses and is equal to the electrical consumption of the motor. This is the reason why the integrated motor compressor flange-to-flange efficiency appears lower than conventional compressor efficiency. From a customer perspective, it means that the comparison between conventional and integrated motor compressor technologies shall be based on the effective electrical respective consumptions and not on the flange-to-flange performances.

As described in this paper, ASME PTC-10 standard (1997) does not provide the type 2 testing conditions and requirements for integrated electrical motor compressors. Therefore, if the customer does not select ASME PTC-10 type 1, it is essential to properly simulate the electrical motor, including its cooling system during the ASME PTC-10 type 2 test. This paper proposes an interpretation of ASME PTC-10 type 2 adapted to integrated electrical motor compressors.

NOMENCLATURE

Magnetic bearing and mechanical parameters

D	= Bearing diameter
L	= Bearing length
A_g	= Active surface normal to the coil
P	= Bearing specific pressure
W	= Supported weight
B_{sat}	= Saturation flux density
μ_0	= Magnetic permeability of air
N	= Number of turns in the coil
X_0	= No min al air gap
I_0	= No min al coil current (Bias current I_{bias} ± Steady current I_c)
L_0	= Small displacement coil inductance
R	= Coil electrical resistance
x(t)	= Air gap variation
i(t)	= Current variation
U(t)	= Amplifier voltage
$\varphi(t)$	= Magnetic flux in air gap

APPENDIX A

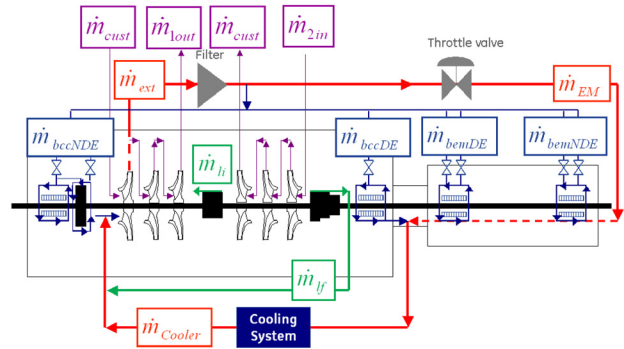*Mass Flow Definition*

Figure A-1 shows the mass flow definition.

Figure A-1. Mass Flow Definition.

$\dot{m}_{cust}$	=	Customer mass flow
$\dot{m}_{1in}$	=	Compressor stage 1 inlet mass flow
$\dot{m}_{1out}$	=	Compressor stage 1 discharge mass flow
$\dot{m}_{2in}$	=	Compressor stage 2 inlet mass flow
$\dot{m}_{2out}$	=	Compressor stage 2 discharge mass flow
$\dot{m}_{ext}$	=	Cooling mass flow extraction
$\dot{m}_{li}$	=	Intermediate balance drum leakage mass flow
$\dot{m}_{lf}$	=	Final balance drum leakage mass flow
$\dot{m}_{EM}$	=	Electric motor cooling mass flow
$\dot{m}_{bccNDE}$	=	Nondriving end compressor bearing (and thrust) cooling mass flow
$\dot{m}_{bccDE}$	=	Driving end compressor bearing cooling mass flow
$\dot{m}_{bemNDE}$	=	Nondriving end electrical motor bearing cooling mass flow
$\dot{m}b_{emDE}$	=	Driving end electrical motor bearing cooling mass flow
$\dot{m}_{Cooler}$	=	Cooling return line mass flow

$\dot{m}_{1in} = \dot{m}_{2out} = \dot{m}_{cust}$, Assuming same flow in stage 1 and stage 2
$\dot{m}_{1out} = \dot{m}_{2in} = \dot{m}_{cust} + \dot{m}_{lf} + \dot{m}_{li}$
$\dot{m}_{ext} = \dot{m}_{bemNDE} + \dot{m}_{bemDE} + \dot{m}_{bccDE} + \dot{m}_{bccNDE} + \dot{m}_{EM}$
$\dot{m}_{Cooler} = \dot{m}_{bemNDE} + \dot{m}_{bemDE} + \dot{m}_{bccDE} + \dot{m}_{EM}$

Pressure and Temperature Definition
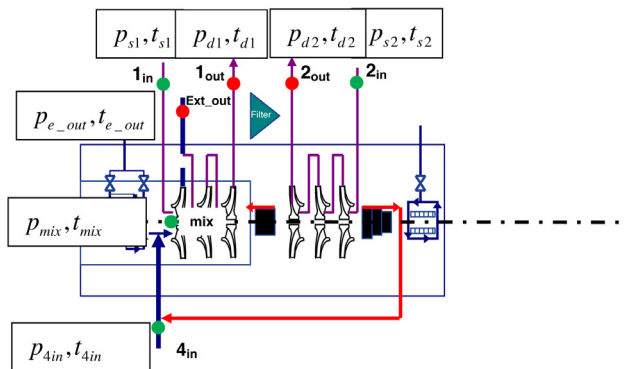
Figure A-2 shows the pressure and temperature definition.

Figure A-2. Pressure and Temperature Definition.

p_{s1}	=	Stage 1 suction pressure
p_{d1}	=	Stage 1 discharge pressure
p_{s2}	=	Stage 2 suction pressure
p_{d2}	=	Stage 2 discharge pressure
p_{mix}	=	Stage 1 first impeller suction pressure
p_{e_out}	=	Stage 1 cooling extraction pressure
p_{4in}	=	Stage 1 cooling return pressure

t_{s1} = Stage 1 suction temperature
t_{d1} = Stage 1 discharge temperature
t_{s2} = Stage 2 suction temperature
t_{d2} = Stage 2 discharge temperature
t_{mix} = Stage 1 first impeller suction temperature
t_{e_out} = Stage 1 cooling extraction temperature
t_{4in} = Stage 1 cooling return temperature

Power and Enthalpy

P = Integrated sealed compressor power
P_1 = Stage 1 gas power
P_2 = Stage 2 gas power
P_{Motor} = Electrical motor losses power
P_{cooler} = Optional cooler removed power
$P_{heating}$ = Heating power introduce through balance line in stage 1
$P_{leakage}$ = Compressor internal leakage power

$P_{Similitude}$ = Integrated sealed compressor power in similitude condition
P_{heater} = Heating power introduce in stage 1 during similitude condition to simulate electrical losses

Subscript "_sim" refers to similitude condition

H_{1in} = Compressor stage 1 inlet flange enthalpy
H_{1out} = Compressor stage 1 discharge flange enthalpy
H_{2in} = Compressor stage 2 inlet flange enthalpy
H_{2out} = Compressor stage 2 discharge flange enthalpy
H_{3out} = Motor main cooling upstream enthalpy
H_{3in} = Motor and motor bearing downstream enthalpy

H_{4out} = Motor bearing cooling upstream enthalpy
H_{4in} = Stage 1 extraction downstream enthalpy
H_{5out} = Optional cooler upstream enthalpy
H_{fext} = Stage 1 extraction upstream enthalpy
H_{4in} = Stage 1 extraction downstream enthalpy

Subscript "_sim" refers to similitude condition

REFERENCES

API Standard 617, 2002, "Axial and Centrifugal Compressors and Expander-Compressors for Petroleum, Chemical and Gas Industry Services," Seventh Edition, American Petroleum Institute, Washington, D.C.

ASME PTC-10, 1997, "Performance Test Code on Compressors and Exhausters," American Society of Mechanical Engineers, New York, New York.

ISO/DIS 14839-2, 2004, "Mechanical Vibration-Vibration of Rotating Machinery Equipped with Active Magnetic Bearings—Part 2: Evaluation of Vibration," International Organization for Standardization, Geneva, Switzerland.

BIBLIOGRAPHY

Habermann, H., "Fonction guidage en rotation, Paliers magnétiques," *Techniques de l'ingénieur*, B 5 345.

Maslen, E., Hermann, P., Scott, M., and Humphris, R. R., 1989, "Practical Limits to the Performance of Magnetic Bearings: Peak Force, Slew Rate, and Displacement Sensitivity," ASME *Journal of Tribology*, 111/331.